Journal of Engineering and Applied Sciences 13 (13): 4924-4931, 2018
ISSN: 1816-949X

Implementation of Upgraded Single-Switch High Boost Converters with Infused Transformer Voltage Incremental Cell

D. Selvabharathi, K. Selvakumar, R. Palanisamy, D. Karthikeyan and K. Vijayakumar
Department of Electrical and Electronics Engineering (EEE),
Sri Ramaswamy Memorial (SRM) University, Chennai, India

Abstract: In this study, a voltage incremental circuit is used to give a universally derivates on developed high step-up converters for high voltage multiplication circuits. N number of one-switch high step-up converters with infused transformer voltage multiplier cell gives us with many advantages, consisting of very high voltage conversion ratio, reduced voltage stress, effective diode reverse-recovery scheme, includes soft-switching operation. The turn's ratio of the infused transformer gives the adjustability to extend the voltage gain. Keeping the active clamp counterpart as a reference, one IGBT reduces the difficulties of the circuit, thereby increasing reliability and stability. Here, the circuit is analyzed with both higher level and lower resonant conditions with the provided key parameters. Incorporation of Pi-filter (LC filter) reduces the ripple content in output. Ultimately, the experimentally obtained results for a 600 W 46-480 V designed prototype are furnished in contributions in this study.

Key words: Built in transformer, high step-up, voltage multiplier cell, effective, scheme, India

INTRODUCTION

The usual boost converter does the function of multiplying voltage. The conventional boost convertor achieves the voltage multiplication through the ideal CCM mode by varying the duty cycle (Do, 2010) but however, the increase in voltage is possible only 4 times the supply voltage shown in Fig. 1.

There are some applications where a 10 fold increase in voltage is required. We can give can quote an example related to the automobile applications which uses the very high intensity light usually need to convert 20 V on battery back up to 300 V at steady state nominal operation, even to 350 V during the start-up stage (Garcia *et al*., 2003). Normal 50-60 V supply systems like batteries are used in the transport applications but likely it has to boost up more than ten times of its output in order to meet the intensity need. Furthermore, the output voltage of the individual Photovoltaic (PV) cell is generally lower than 70 V (Shenkman *et al*., 2004; Erickson and Maksimovic, 2001). However, the AC voltage at the grid side is 220 V for single-phase local utility in the country which also calls for high step-up and high-efficiency converters to realize the integrated PV modules:

$$\text{Power} = \text{Voltage}*\text{Current}$$

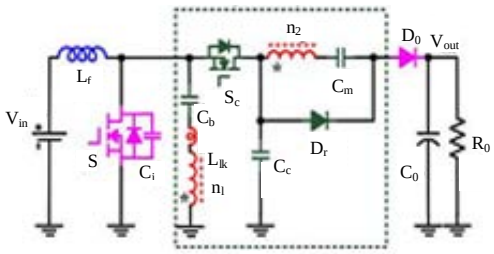

Fig. 1: Voltage multiplier cell

Assuming power = 200 W and voltage as 50 V, the current will be 4 A. Now, if a Voltage of 100 V is needed then the current reduces to 2 A in order to maintain the same 200 W power. It is clearly visible that on increasing the voltage profile, the current profile has to be reduced in order to maintain the same power rating.

Now, the question arises as to why current profile is not changed instead of voltage profile? It is because a voltage multiplication is needed, here in motors with the increase in load it draws more current, i.e. with increase in load the current levels increase. So, in motors the current profile is increasing but what is needed is increase in voltage profile. The best example for increase in voltage profile is a car's headlight where an increase in voltage in seen as illumination.

Corresponding Author: D. Selvabharathi, Department of Electrical and Electronics Engineering (EEE),
Sri Ramaswamy Memorial (SRM) University, Chennai, India

Also, the conventional boost convertor uses multiple switches to achieve the voltage gain. This results in additional switching losses thereby reducing efficiency. Switch operating condition and the diode reverse-recovery condition are plays a vital role in the high output voltage loads. A Zero Voltage Switching (ZVS) Zero Current Switching (ZCS) boost converter with voltage multiplier circuits are developed to minimize the switching losses (Santhoshi *et al*., 2016). The major limitations of the converters published by Vijayalakshmi *et al*. (2016) and Puviarasi and Dhanasekaran (2015) is that these topologies cannot provide another controllable and user free concepts except the change in duty pulse to obtain the large and wide voltage conversion that limitations are overcome by the new topology derived.

The novel idea revels from the new topology is used to overcome the above difficulties related to switching losses by means of new soft switching methods and an improved pulse width modulation techniques. With the help of this ZVS soft switching techniques the smooth operation of the circuits can be achieved due to this the stress across each switch can be balanced in the other hand we are using ZCS techniques, so, the switching stress at the point of circuit off condition can be reduced. The voltage multiplication by single cell can be achieved by voltage multiplier circuits. Either it may be of voltage doublers, tripler quadruples. This can be achieved by fly back capacitor circuits. In this regards, we have to large number of capacitors in turn one single switch to achieve.

MATERIALS AND METHODS

Topology derivation and circuit operational analysis: The stimulation of proposed ZVS high step-up built-in transformer based converter by Bharathi and Sasikumar (2016) is shown in Fig. 2. The boosting in voltage multiplier cell is composed of a transformer an active clamp switch S_c, a clamp capacitor C_c, a DC block capacitor C_b, a switched capacitor C_m and a regenerative diode D_r. The switches S and S_c work with the un symmetrical reverse operation to regulate the output Cc. ZVS soft-switching performance is achieved for the switches S and Sc due to the additional parallel capacitor Cs. The input current ripple is small due to its CCM operation to remove the large input electrolytic capacitors. As a result, this built-in transformer based converter is a best converter for the high step-up and more efficiency transfer systems.

From the above concept the capacitor is charged to the maximum and clamps to the maximum towards the of

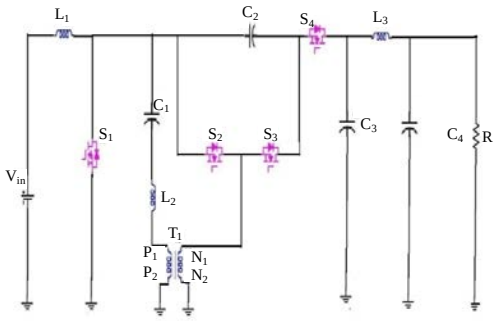

Fig. 2: Proposed high step-up converter

input voltage and it discharges to load with the limited switching time leads to the low switching frequency. The improved single-switch high step-up converter is introduced. This improved version has some other clearly advantageous performance which will be discussed in detail in the following sections. In the dashed block, a voltage multiplier cell is inserted to extend the voltage gain and reduce the switch voltage stress.

Here, we are using a infused transformer with different types of primary and secondary turns. With respect to the turns conditions of primary and secondary winding the boosting level are improved infuse to achieve the above incremental condition over resonance frequency and below resonance frequency conditions are used open switch uses the over resonance condition and closed switch uses the below resonance conditions. Due to the above category the leakage inductance value can be reduced at the point of transformer.

Part 1 [t_0, t_1]: When switch t_1 is in on condition, the semiconductor S will be in the running state and the voltage transfer towards the filter inductor L_f is V_{in} . The clamp diode and the output rectifier Do are developed by the update mathematical analysis Eq. 1-3:

$$V_{ts} = V_{cm} - V_{cc} \tag{1}$$

$$L_{lk}\frac{di_{LK(t)}}{dt} = V_{tp} - V_{cb(t)} \tag{2}$$

$$i_s(t) = i_{lf}(t) + i_{Lk}(t) + \frac{i_{LK(t)}}{N} \tag{3}$$

Part 2 [t_1, t_2]: In the point of t_1, the I of the leakage inductance L_{lk} resonates (Wu *et al*., 2008) towards the zero and the regenerative diode Dr turns OFF automatically, this gives the information about the reverse-recovery losses. The inductor I is still developing gradually due to the input voltage.

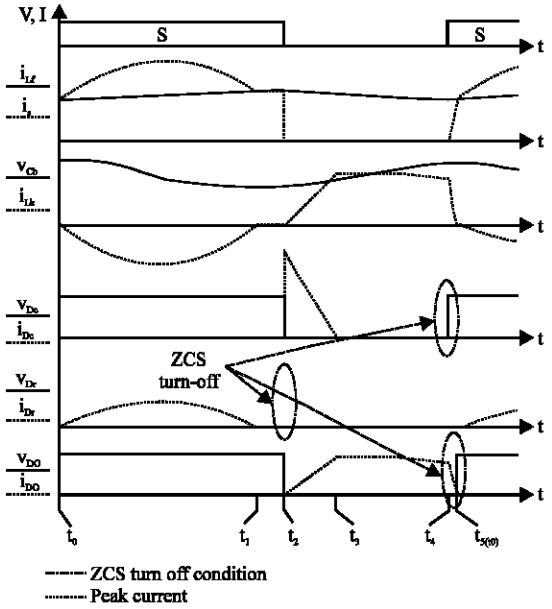

Fig. 3: Stage of switching output

Part 3 [t_2, t_3]: At t_2 , the switch S turns OFF and then the clamp diode Dc and the output rectifier Do turn ON to gives out by means of the current equation given as:

$$i_D(t) = \frac{i_{LK(t)}}{N} \quad (4)$$

The operation of each stage of switching output and its modes of operation are shown in Fig. 3 and 4.

Voltage and current stress analysis of power semiconductor switches: The voltage stresses of the semiconductor S and the clamping diode Dc are equal to the voltage on the clamping capacitor Cc:

$$V_s = V_{dc} = V_{cc} = \frac{V_{in}}{1\text{-}D} = \frac{V_{out}}{N+2} \quad (5)$$

From Eq. 6, it can be given as that the voltage stress across the switch is decreased to the maximum as the turn's ratio move towards the maximum which makes high performance MOSFETs with low RDS ON available to increase the circuit actions in a better way (Vijayalakshmi *et al*., 2016). The maximum switching voltage is only half of the high output voltage. The voltage stress of the regenerative diode Dr is the same as that of the output diode Do which is equal to the output voltage minus the clamp capacitor voltage:

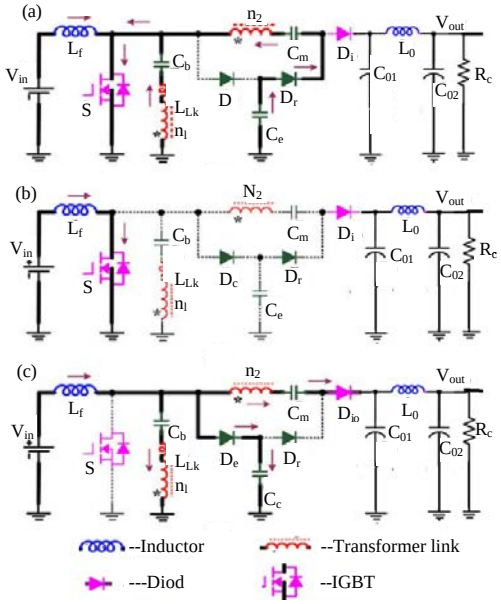

Fig. 4: a-c) Mode of operation output

$$V_{Do} = V_{Dm} = V_{out} - V_{co} = \frac{N+1}{1\text{-}D} V_{in} = \frac{N+1}{N+2} V_{out} \quad (6)$$

As a result, the average current of the diodes, Dr and Do is the same. In order to simplify the analysis, the switch turn-ON period is assumed to be half of the resonant period which is given as DTs ˜Tr /2. The peak current of the diodes Dc, Dr and Do can be derived by Eq. 7 and 8:

$$I_{Dc_{peak}} \approx I_{in} \approx \frac{(N+2)}{(1\text{-}D)} I_{out} \quad (7)$$

$$I_{Dr_{peak}} \approx \frac{piT}{T} I_{out} \approx \frac{pi}{2D} I_{out} \quad (8)$$

$$I_{Do_{peak}} \approx \frac{I_{Lf}}{N+1} \approx \frac{I_{in}}{N+1} \approx \frac{(N+2)}{(N+1)(1\text{-}D)} I_{out} \quad (9)$$

And the switch peak current and RMS current are calculated by Eq. 9-11:

$$I_{s_{peak}} \approx I_{in} + \frac{piTs}{Tr} I_{out} \approx \frac{(N+2\text{-}pi)D+pi}{2(1\text{-}D)D} I_{out} \quad (10)$$

$$\frac{1}{Ts} \int_0^{\frac{Tr}{2}} \left[\left(\frac{N+1piTsI_{out}}{Tr} \right) \sin(Wrt) + lin \right) \quad (11)$$

From the static analysis operation, it can be routed from the clamp diode current is reduced to zero before it

turns OFF that gives an output related to no reverse-recovery problem for the clamp diode. For the output diode, its turn-OFF current dragging rate is controlled by the inductance leakage of the inbuilt-transformer which is sated by Eq. 12:

$$\frac{di_{Do}(t)}{dt} = \frac{(N+1)V_{out}}{N(N+2)L_{lk}} \quad (12)$$

For the condition of regeneration, there are two different cases lies based on the operation modes. In O_{rf} operation, the current across the regenerative diode is resonated towards zero before it turns OFF without any recovery problem. In B_{rf} mode, its turn-OFF current falling rate is given by Eq. 13:

$$\frac{di_{dr(t)}}{dt} = \frac{V_{out}}{(N+2)L_{kk}} \quad (13)$$

From Eq. 13, it can be coated that the reverse-recovery problem can be sifted effectively by shifting a small leakage inductance as the turn's ratio increases, which can decreases the electromagnetic interference noise and develop the circuit efficiency.

RESULTS AND DISCUSSION

Circuit performance comparison and evaluation: In a nutshell, the next solution is to introduce the built-in transformer where its change in turns ratio is used to control and convert the output voltage. Added to it the switched capacitor technique can be added with the coupled inductor or in built-transformer to derive improved high step-up converters (Puviarasi and Dhanasekaran, 2015) which can further increase the voltage gain and reduction in switching voltage stress.

Related to the nowadays publication of journals, the coupled inductor-based high step-up converters can be related to the summation of the coupled inductor and switched capacitor techniques (Devikar *et al*., 2016; Bharathi and Sasikumar, 2016) which can be derived by the voltage doubler, tripler and quadruple and by using this circuits adding in a cascaded manner more boosting voltage can be attached with the concepts of reduced switching losses, the switch voltage stress can be reduced correspondingly. Addition to, it the leakage energy can be processed by employing active filter scheme which cannot only suppress the possible turn-OFF voltage spikes on the power MOSFETs but also provide ZVS or ZCS soft-switching operation.

Consequently, a trade-off should be made to optimize the converter performance (Devikar *et al*., 2016) based on the application specifications. In the recent trend, renewable energy plays a vital role in the production of electricity. In this regards, PV plays a major role but the power transfer from the PV need a voltage boosting circuit, so that, it can feed with a constant rated voltage towards the load, the conventional multiplier circuits are very bulky with separate transformer and large number of switch's in turn the cost control is going to be higher in this proposed system all the drawbacks are overcome by using the built in transformer here, the basic concepts of inductor charging and discharging are used by the way the voltage doubler, tripler quadruple concepts are achieved by means of a single switch.

Design analysis of key parameters

Turns ratio selection in built in transformer: The determination of duty cycle is decided by the turn's ratio of the transformer and it determine the switching and voltage rate, the stress across each switch is designed by the turns ratio only given by Eq. 14:

$$N = \frac{V_{out}}{V_{in}\ (1\text{-}D)\text{-}2} \quad (14)$$

Design of leakage inductance parameter present in built in transformer: Leakage inductance relation is given and the diode current falling rate is derived by Eq. 15:

$$\frac{di_{Do(t)}}{dt} = \frac{(N+1)V_{out}}{N(N+2)L_{Lk}} \quad (15)$$

Selection of input inductor towards filter: The input filter inductor Lf is designed to make that the input current ripple is approximately 20% of the average input current. This is derived by Eq. 16:

$$L_f = \frac{V_{in}D}{\Delta I_{Lf} fs} \quad (16)$$

Due to the built-in voltage multiplier cell of the proposed converter (Wu *et al*., 2008), the switch duty cycle can be optimized to reduce the input current ripple which can prolong the usage life of the PV arrays or the fuel cells.

Power device selection: The voltage and current rating of the load decides the power supply circuits. It may be varies with raise in load vice versa.

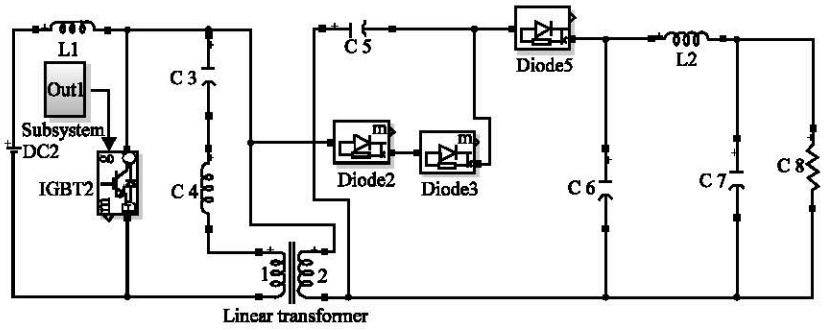

Fig. 5: Voltage multiplier cell converter simulation diagram

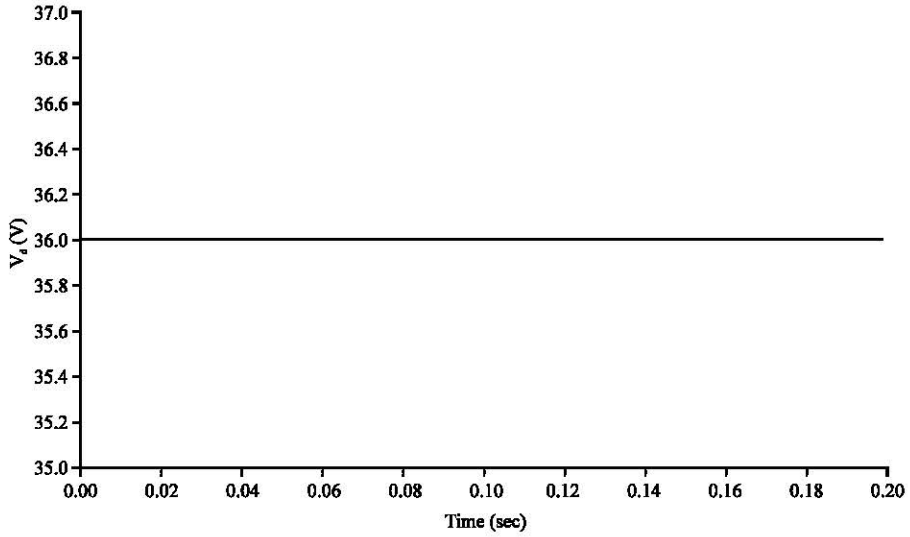

Fig. 6: DC input voltage waveform

Design of capacitor: Consideration for the capacitor design. The relationship between the voltage ripple and the output power can be derived by Eq. 17:

$$C \geq \frac{P_{out}}{V_{outΔVcF}} \quad (17)$$

where, Δvc is the maximum applicable voltage ripple on the capacitor Cc or Cm. The different operating of the circuits results decides the value of blocking capacitor.

Simulation of voltage multiplier cell: The resonant converter circuit with voltage multiplier cell diagrams is shown in Fig. 5 and the corresponding output results are obtained below. Figure 6 represents the DC input voltage waveform. Figure 7 represents the wave form VG, ID and IDS across each switch for proposed system. Figure 8 represents the DC output voltage waveform (380 V). Figure 9 represents the power output wave form (500 W). Figure 10 represents the DC output current wave form (1.1 A).

Efficiency of the proposed converter: The measured efficiency of the proposed converter is plotted and the maximum efficiency of 96.6% on the other side the of conventional circuit efficiency of 95.6% at 500 W max loads are obtained with Cb = 6.9 μF. The resulted efficiency comparison with different input voltages and Cb = 6.9 μF is given in Fig. 11.

It can be seen that even the input voltages have a large variations shown in Fig. 12. Within a large load range the conversion efficiency can be kept up to a high level. The maximum efficiency is still over 96% even though the input voltage is reduced to 30 V.

Hardware prototype: By using the various components with the specified parameters cited in Table 1. The

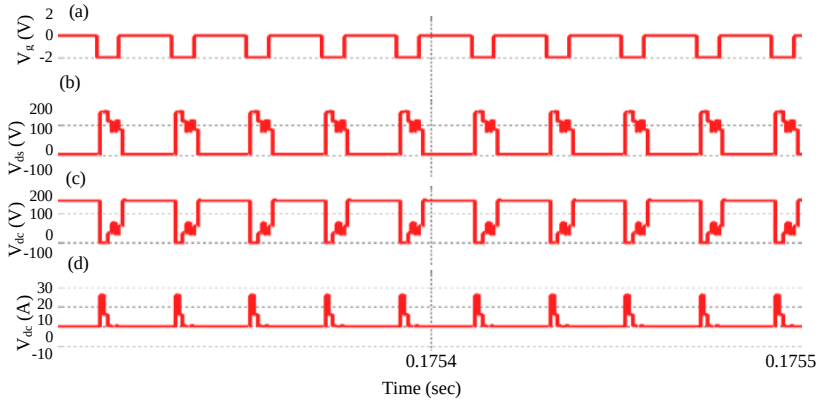

Fig. 7: a-d) Wave form VG, ID and IDS across each switches for proposed system

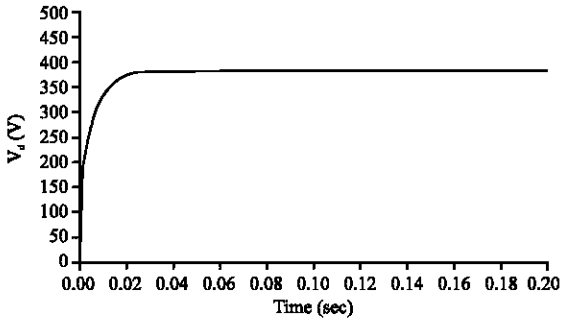

Fig. 8: DC output voltage waveform (380 V)

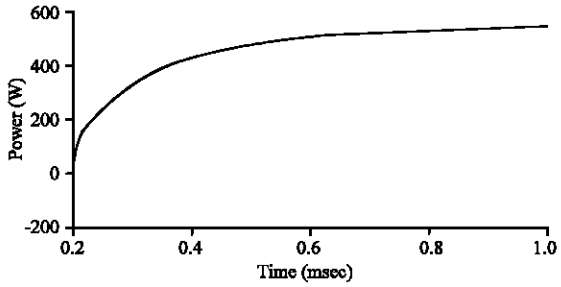

Fig. 9: Power output waveform (500W)

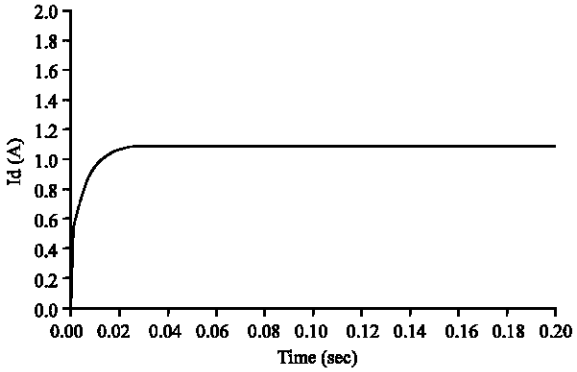

Fig. 10: DC output current waveform

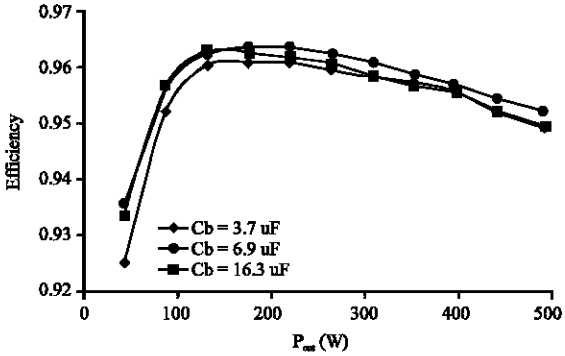

Fig. 11: Efficiency comparison for C, LC and Pi filter

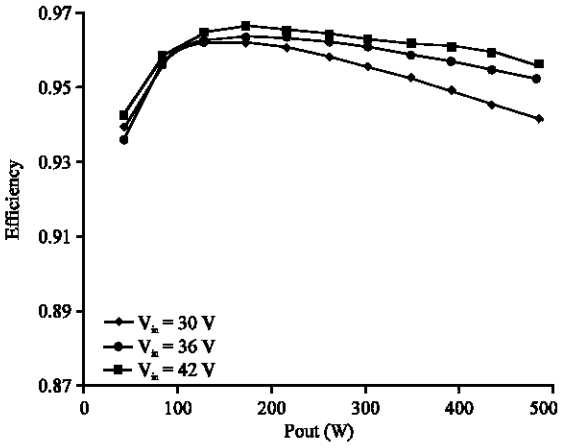

Fig. 12: Efficiency comparison for different input voltage Cb = 6.9 μF

prototype hardware model was developed and its was executed with practical condition of input voltage and the boosting voltage N times was achieved and is proved. The details of hardware prototype are shown in Fig. 13-15.

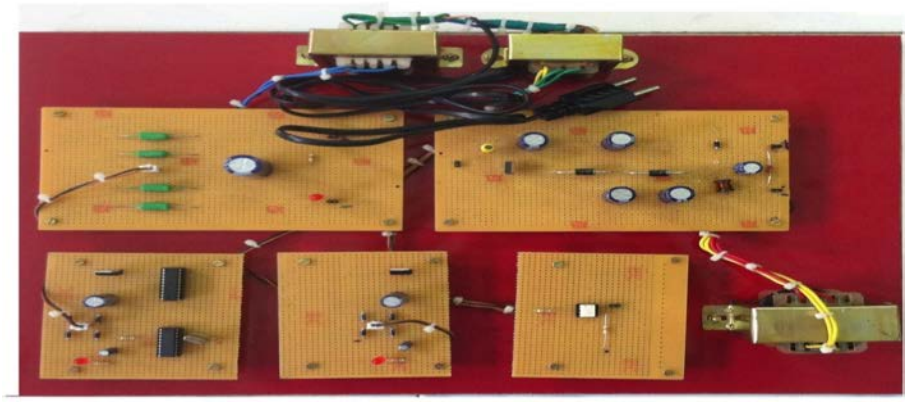

Fig. 13: Prototype

Fig. 14: Input voltage-prototype result

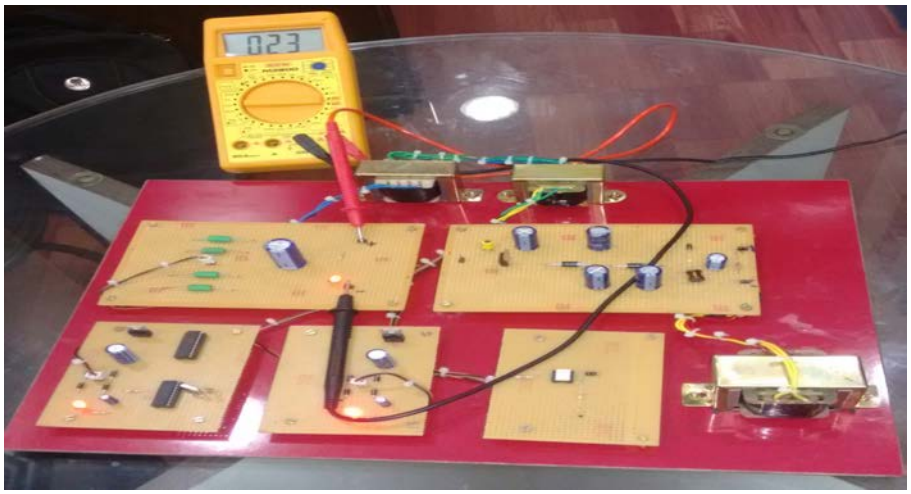

Fig. 15: Output voltage-prototype result

Table 1: Components and parameters of prototype

Components	Parameters
Vin input voltage	23V
Vout (output volatge)	241V
Pout maximum output power	500 W
Fs (switching frequency)	100 kHz
Lf (input filter inductor)	100 μ Henry
Turns ratio	17/7
Lm magnetizing inductor	260 μ Henry
LLK leakage inductor	1.6 μ Henry
S power MOSFET	IRFP4227
DC clamp diode	MUR820
Dr and Do diode	MURI560
Cc clamp capacitor	2.2 μF
Cb block capacitor	3.7,6.9 or 16.3 μF
Cm switched capacitor	1 μ F
Co1 (output capacitor 1)	100 μF
Co1 (output capacitor 2)	100 μF
Lo (output inductor	57 μ Henry
Ro (load resistor)	350 Ω

CONCLUSION

The infused transformer-less single cell boost converter was stimulated using ZCS resonant techniques with the help of MATLAB tool and the results are compared with the various types of filter such as C, PI and LC filter and the efficiency comparison was done with various profiles like voltage, current and power including the amount of THD and finally conclude that the PI filter sounds good in the comparison of all profile and the comparison results leads in the development of hard ware of one switch voltage builder with PI filter. The result output proves the above statement.

REFERENCES

Bharathi, K. and M. Sasikumar, 2016. Voltage compensation of smart grid using bidirectional intelligent semiconductor transformer and PV cell. Indian J. Sci. Technol., 9: 1-8.

Devikar, R.N., D.V. Patil and V. Chandraprakash, 2016. A soft computing approach to improve the network performance. Indian J. Sci. Technol., 9: 1-8.

Do, H.L., 2010. A soft-switching DC-DC converter with high voltage gain. IEEE. Trans. Power Electron., 25: 1193-1200.

Erickson, R.W. and D. Maksimovic, 2001. Fundamentals of Power Electronics. 2nd Edn., Wolters Kluwer, New York, USA., ISBN:0-7923-7270-0, Pages: 883.

Garcia, O., J.A. Cobos, R. Prieto, P. Alou and J. Uceda, 2003. Single phase power factor correction: A survey. IEEE. Trans. Power Electron., 18: 749-755.

Prasanthi, G., V. Sumalatha and A. Sudheer, 2010. Optimum design of boost converter for charging the battery by non-conventional energy source. Indian J. Sci. Technol., 3: 724-726.

Puviarasi, R. and D. Dhanasekaran, 2015. Interleaved boost converter fed DC machine with zero voltage switching and PWM technique. Indian J. Sci. Technol., 8: 376-382.

Santhoshi, B.K., K.M. Sundaram, M. Sivasubramanian and S. Akila, 2016. A novel multiport bidirectional dual active bridge DC-DC converter for renewable power generation systems. Indian J. Sci. Technol., 9: 1-4.

Shenkman, A., Y. Berkovich and B. Axelrod, 2004. Novel AC-DC and DC-DC converters with a diode-capacitor multiplier. IEEE. Trans. Aerosp. Electron. Syst., 40: 1286-1293.

Vijayalakshmi, M., R. Ramaprabha and G. Ezhilarasan, 2016. Design of auxiliary resonant boost converter for flywheel based photovoltaic fed microgrid. Indian J. Sci. Technol., 9: 1-6.

Wu, T.F., Y.S. Lai, J.C. Hung and Y.M. Chen, 2008. Boost converter with coupled inductors and buck-boost type of active clamp. IEEE. Trans. Ind. Electron., 55: 154-162.